Journal of Controlled Release 323 (2020) 179–190

Contents lists available at ScienceDirect

Journal of Controlled Release

journal homepage: www.elsevier.com/locate/jconrel

Biodegradable nanoparticles decorated with different carbohydrates for efficient macrophage-targeted gene therapy

Qijing Chen[a,1], Mingzhu Gao[a,1], Zhongyu Li[b], Yue Xiao[a], Xin Bai[a], Kofi Oti Boakye-Yiadom[a], Xiaoyang Xu[b,*], Xue-Qing Zhang[a,*]

[a] Engineering Research Center of Cell & Therapeutic Antibody, Ministry of Education, and School of Pharmacy, Shanghai Jiao Tong University, 800 Dongchuan Road, Shanghai 200240, PR China
[b] Department of Chemical and Materials Engineering, New Jersey Institute of Technology Newark, NJ 07102, USA

ARTICLE INFO

Keywords:
Macrophage-targeting nanoparticles (NPs)
Gene delivery
Nanomedicine
Carbohydrate decoration

ABSTRACT

Macrophages are attractive therapeutic targets due to their contributions to many pathological processes including cancers, atherosclerosis, obesity, diabetes and other inflammatory diseases. Macrophage-targeted gene therapy is an effective strategy for regulating macrophage function at the site of inflammation to treat related diseases. However, macrophages are recognized as difficult to transfect cells and non-specific delivery would inevitably cause unwanted systemic side effects. Herein, we prepared a series of macrophage-targeted nanoparticles (NPs) using cationic lipid-like compound G0-C14 and different carbohydrates-modified poly(lactide-*co*-glycolide) (PLGA) or poly(lactide-coglycolide)-*b*-poly(ethylene glycol) (PLGA-PEG) for gene delivery by a robust self-assembly method. The yielded NPs were decorated with carbohydrate-based targeting moieties including mannose, galactose, dextran, and a mixture of mannose and galactose. EGFP messenger RNA (mRNA) and GFP plasmid DNA (pDNA) were used as reporter genes to evaluate NP-mediated gene transfection in macrophages. Experimental results of macrophage phagocytosis demonstrated that more carbohydrate-decorated NPs were endocytosed by Raw 264.7 cells than the ones without carbohydrate modification. Mannose-decorated NPs showed better targeting ability to macrophages than NPs decorated with galactose only and a blended mixture of mannose and galactose. It is worth noting that polysaccharide dextran-modified NPs also exhibited evident targeting effects. CCK-8 assay revealed that no cytotoxicity was observed for all tested NP concentrations up to 2.8 mg/mL. The carbohydrate-decorated polymer/G0-C14 exhibited strong entrapment of mRNA and pDNA with an encapsulation efficiency of above 95%. The targeted NPs significantly improved cellular internalization and transfection efficiency in macrophages, depending on the type and content of the carbohydrate moieties presented on the NP surface. Interestingly, dextran-decorated NPs showing higher endocytosis at various concentrations in macrophages also demonstrated more efficient mRNA transfection, suggesting that the NP-mediated mRNA transfection efficiency was consistent with the endocytosis results.

1. Introduction

Macrophages are a critical component of the innate immune system and have a crucial role in tissue homeostasis and immunity, and they contribute to many pathological processes including cancers, fibrotic lung disease, cardiac disease, inflammatory disorders, and a variety of infectious diseases, including HIV-1 [1]. Generally, macrophages have two important subpopulations: “classically activated macrophages” (M1) and “alternatively activated macrophages” (M2) which are present in the inflammatory environments of various diseases such as solid tumors, type II diabetes and atherosclerosis. M1s and M2s are thought to be responsible for different functions in these microenvironments. For example, in the tumor microenvironment, M2 macrophages are notorious for suppressing tumor immunity and promoting vascularization, in contrast to M1s which destruct and phagocytose tumor cells [2]. However, in type II diabetes, M2s play an important role in the development of islets, especially in the proliferation and differentiation of islet β cells. Instead, proinflammatory factors (*e.g.* IL-1β and TNF-α) produced by M1s promote the function of islet β cell damage [3]. In the context of atherosclerosis, the long-term inflammatory response caused by the macrophage-driven defection of inflammation resolution is also the main pathogenic factor [4,5]. Since macrophage function is widely

* Corresponding authors.
E-mail addresses: xiaoyang.xu@njit.edu (X. Xu), xueqingzhang@sjtu.edu.cn (X.-Q. Zhang).
[1] These authors contributed equally to this work.

https://doi.org/10.1016/j.jconrel.2020.03.044
Received 20 December 2019; Received in revised form 22 March 2020; Accepted 28 March 2020
Available online 22 April 2020
0168-3659/

associated with the response to a number of disease states, macrophages are attractive therapeutic targets to treat a broad spectrum of pathologies. In this context, it is crucial to develop an efficient delivery platform capable of targeting and modulating the function of macrophages at the site of inflammation, which would be a promising therapeutic approach for the treatment of a broad range of diseases.

Gene transfection assays are an effective tool to analyze and adjust macrophage functions at the molecular level. For example, tumor-associated macrophages (TAMs) are notorious for suppressing tumor immunity and promoting vascularization. In this case, it has been shown that TAM immune responses and antitumor immunity could be activated through inserting therapeutic genes [6]. However, gene transfection in macrophages is difficult due to intracellular reactive oxygen species and endosomal degradation of genes. Although viral vectors are popular due to their high gene transfection efficiency, safety risks associated with viral vectors due to off-target immunogenicity, inflammatory response and toxicity are concerns which hinder their widespread usage [7]. To overcome this challenge, non-viral gene transfer methods such as calcium-phosphate precipitation, DEAE-dextran, particle bombardment, and electroporation have been developed to improve macrophage transfection [8]. However, these methods are associated with low gene transfection efficiency or high cytotoxicity. In addition, non-viral gene vectors based on cationic lipids and polymers (*e.g.* polyethyleneimine, liposomes, and poly(*β*-amino esters)) have also been pursued and have proved to be effective gene transfection carriers in many cells but not macrophages [9–12].

In general, macrophages possess high phagocytic capability to indiscriminately internalize micro/nanoparticles due to their primary role in clearing cellular debris, pathogens, and foreign substances. In addition to the above passive targeting of macrophages, there are also many targeting ligands being investigated pre-clinically for active targeting such as mannose [13], folic acid [14], legumain [15], transferrin and M2 macrophage-targeting peptide (M2pep) [16]. Among them, the biocompatibility and specific receptor recognition ability make carbohydrates useful as potential targeting ligands for macrophage-targeted drug and gene delivery applications. It has been reported that the gene transfection efficiency in macrophages could be significantly increased by mannosylated lipoplexes [17,18], poly(L-lysine) [19], cationic solid lipid NPs [20], chitosan NPs [21], polyamidoamine and polyethylenimine [22] in comparison with the corresponding unmodified vectors. In addition to macrophage mannose receptor (MMR, cluster of differentiation 206, CD206), macrophages also express other carbohydrate receptors, such as macrophage galactose-binding lectin (MGL, CD301). Mannose and galactose have been used to conjugate with drugs or vaccines to modulate or potentiate the immune response [23]. As the first and only FDA-approved macrophage-targeted lymphatic mapping agent, the mannose conjugate Lymphoseek® (technetium Tc 99m tilmanocept) can specifically target the CD206 mannose receptor expressed on activated macrophages [24]. In addition to monosaccharides, a polysaccharide of dextran was also proved to be able to efficiently target adipose macrophages in obese mice [25]. However, most of the macrophage-targeted vectors were used as imaging agents or to deliver small molecular drugs, but their use for delivery of biomacromolecules especially nucleic acids (*e.g.* mRMA or pDNA) were rarely reported.

Before, we have developed a hybrid NP platform through self-assembly of a biodegradable poly(lactide-coglycolide)-*b*-poly(ethylene glycol) (PLGA-PEG) diblock copolymer and a self-synthesized cationic lipid-like molecule designated as G0-C14 [26]. The G0-C14 is composed of a cationic head group that can efficiently entrap therapeutic nucleic acids *via* electrostatic interactions and a flexible hydrophobic tail for self-assembly with PLGA-PEG to form NPs. The cationic head group includes many primary amine, secondary amine, and tertiary amine groups which exert strong buffering capacity to induce a proton-sponge effect and release payloads into the cytosol. The proton-sponge effect of G0-C14 has been proved in previous work [27]. This PLGA-PEG/lipid hybrid NP platform could co-deliver siRNA and cisplatin prodrug and release both payloads in a sustained manner, and exhibited a good therapeutic efficacy against tumor cells. Herein, we successfully optimized the structure of the cationic lipid G0-C14 by adjusting the molar ratio of the dendrimer and 14 carbon tail to facilitate the entrapment and delivery of large nucleic acids (*i.e.* mRNA or pDNA). A series of polymer/lipid hybrid NPs were then prepared by encapsulating the G0-C14/mRNA or G0-C14/pDNA complex using various carbohydrate-modified PLGA or PLGA-PEG polymers *via* nanoprecipitation. The resulting NPs were engineered with different carbohydrates, including mannose, galactose, dextran, and a mixture of mannose and galactose constructed from two sugar-conjugated PLGA-PEG polymers. Flow cytometry was performed to evaluate the cellular uptake of the fluorescently-labeled NPs in macrophages. CCK-8 assay was carried out to study their cytotoxicity. EGFP (enhanced green fluorescent protein) mRNA and GFP (green fluorescent protein) pDNA were used as reporter genes to investigate NP-mediated gene transfection in macrophages. The impact of differing carbohydrate decoration and content of the carbohydrate moieties on the targeting capacity and transfection efficacies of the engineered NPs were also investigated.

2. Materials and methods

2.1. Materials

Carboxy-terminated PLGA [50:50 poly(DL-lactide-coglycolide) (0.55–0.75 dL g^{-1})] was purchased from Lactel Absorbable Polymers. The heterobifunctional PEG polymers NH_2-PEG-OH and NH_2-PEG-SH (molecular weight of 3.4 kDa) were purchased from Laysan Bio, Inc., and BOC-HN-PEG-NHS and PEG (Amino end-capped, 3 kDa) were purchased from JenKem Technology USA. 4-Aminophenyl alpha-D-mannopyranoside (MAN) was purchased from Synthose Inc. 4-Aminophenyl beta-D-galactopyranoside (GAL) was purchased from Shanghai Bide Pharmatech Co., Ltd. *N*-Hydroxysuccinimide (NHS), 1-ethyl-3-[3-dimethylaminopropyl] carbodiimide (EDC) hydrochloride, *N*, *N*-diisopropylethylamine (DIPEA) and trifluoroacetic acid (TFA) were purchased from Beijing Yinuokai Technology Co., Ltd. Dextran (MW = 70 kDa) and polyvinyl alcohol (PVA, MW = 20 kDa) were purchased from Shanghai Maclin Biochemical Technology Co., Ltd. 4-(Dimethylamino)pyridine (DMAP) was purchased from J&K Scientific Ltd., Shanghai, China. Anhydrous pyridine, lithium chloride (LiCl), triethylamine (TEA), anhydrous dimethyl sulfoxide (DMSO), anhydrous dimethylformamide (DMF), mono-boc protected diethylamine (BocEDA) and Cell Counting Kit-8/WST-8 were purchased from Shanghai Mokai Biotechnology Co., Ltd. 4-Nitrophenyl chloroformate (PNC) was purchased from Shanghai Titanchem Co., Ltd. Sulfo-Cyanine5.5 NHS ester and Sulfo-Cyanine5.5 maleimide were purchased from Lumiprobe Corporation. Cationic ethylenediamine core-poly (amidoamine) (PAMAM) dendrimer generation 0 (G0) and 1,2 epoxytetradecane (C14) were purchased from Sigma-Aldrich. Fetal bovine serum (FBS) was purchased from Biyotime Technology. Dulbecco's Modified Eagle Medium (DMEM; Gibco), fetal bovine serum (FBS; Gibco), streptomycin and penicillin (Thermo-Fisher Scientific) were purchased from YingWei Jieji (Shanghai) Trading Co., Ltd.

2.2. Characterization

The structure of the polymers was characterized by ^{1}H NMR analysis run on an Agilent Technologies 500/54 Premium Shielded instrument and a chemical shift was reported with the solvent residue at DMSO-d_6 (2.50), $CDCl_3$ (7.26) or D_2O (4.79) as the reference. Gel permeation chromatography (GPC, EcoSEC HLC-8320) was used to analyze the molecular weights and dispersities of the polymers. DMF containing 0.02 M LiBr was used as the eluent at a flow rate of 1 mL/min, and the temperature of the column was controlled at 50 °C. Dynamic light scattering (DLS) was performed on a Malvern ZS90 at a detection angle

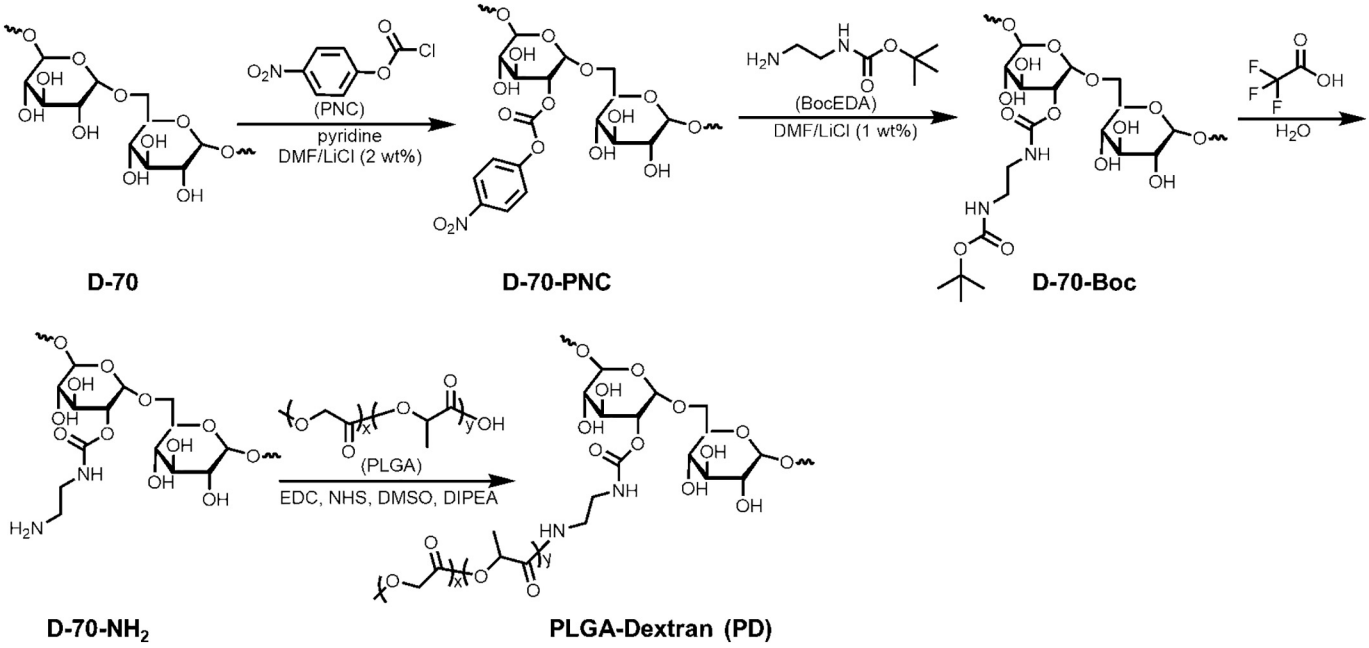

Scheme 1. Synthetic route of PLGA-Dextran (PD).

of 90°. The average diameter and polydispersity were measured at 25 °C and automatically analyzed in the cumulant mode using the Malvern software. The morphology of the NPs was characterized by transmission electron microscopy (TEM, FEI Tecnai G2 Spirit Bio TWIN). The TEM samples were prepared by dripping the NP solutions (1% w/v) onto the copper grid and were stained with 1% uranyl acetate. The fluorescent intensity of RAW 264.7 macrophages was analyzed by flow cytometry (BD LSRFortessa™) and data was analyzed under FlowJo software.

2.3. Experimental

2.3.1. Synthesis of PLGA-Dextran (PD) (Scheme 1)

D-70-PNC. D-70 (1.0 g) and LiCl (2.0 g, 2 w/v % of DMF) were weighed and added into a 150 mL round-bottom flask. Anhydrous DMF (100 mL) was added and stirred for 3 min. The suspension was continuously stirred at 90 °C for 1 h until the suspension became clear. Then the solution was cooled to 0 °C in an ice-water bath and anhydrous pyridine (1.3 mL, 0.015 mol) and PNC (3.11 g, 0.015 mol) were added in sequence. After The solution was stirred at 0 °C for 4 h, and D-70-PNC was obtained by precipitating the solution into cold ethanol, washed with diethyl ether three times, and dried under vacuum for 12 h. Yield: 1.6 g (40%). ^{1}H NMR (DMSO-d_6, 400 MHz): 7.54 and 8.28 ppm (b, aromatic protons), 5.39 and 5.52 ppm (s, dextran glucosidic protons at positions which have nitrophenyl substituents), 4.9, 4.8, and 4.5 ppm (s, dextran hydroxyl protons), 4.7 ppm (s, dextran anomeric proton), 3.19–3.73 ppm (m, dextran glucosidic protons) (Fig. S1).

D-70-Boc. LiCl (1.26 g) was dissolved into 126 mL anhydrous DMF and then D-70-PNC (1.58 g) was added. The mixture was purged with N_2 and stirred until D-70-PNC dissolved. BocEDA (0.351 g, molar ratio of amine to PNC group = 6.5) dissolved in anhydrous DMF (4 mL) was added. The solution was stirred at room temperature for 24 h under N_2 protection. D-70-Boc was obtained by precipitating the solution into cold ethanol, washed with diethyl ether three times, and dried under vacuum for 12 h. Yield: 1.2 g (62%). ^{1}H NMR (DMSO-d_6, 400 MHz): 4.52, 4.86, and 4.93 ppm (s, dextran hydroxyl protons), 4.67 ppm (s, dextran anomeric proton), 3.10–3.89 ppm (m, dextran glucosidic protons), 3.33–3.52 ppm (m, -CH_2-CH_2-), 1.37 ppm (s, -C(CH_3)$_3$) (Fig. S2).

D-70-NH_2. D-70-Boc (1.11 g) was dissolved into 28 mL deionized water containing 9.6% (v/v) TFA. The solution was stirred for 24 h under N_2 and neutralized to pH 7.0 using 4.0 M NaOH. The mixture was dialyzed against water (MWCO 1 kDa). Remove the insolubles and D-70-NH_2 was obtained as a solid white product after lyophilization. Yield: 0.76 g (68%). ^{1}H NMR (D_2O, 400 MHz): 4.81 ppm (s, dextran anomeric proton), 3.31–3.83 ppm (m, dextran glucosidic protons), 2.98 and 3.46 ppm (m, –CH_2-CH_2-) (Fig. S3).

PLGA-Dextran (PD). PLGA (0.2 g) was dissolved into dry DCM (1.5 mL). EDC·HCl (10 mg, 0.05 mmol) dissolved by 0.5 mL dry DCM and NHS (5.7 mg, 0.05 mmol) dissolved by 20 μL DMSO were added in sequence. The solution was stirred at room temperature for 2 h. PLGA-NHS was obtained by precipitated in cold methanol/diethyl ether (50/50 v/v), further washed two times and dried by rotary evaporation. PLGA-NHS was dissolved in dry DMSO (4 mL) and subsequently dextran (0.021 g) was dissolved into the solution. DIPEA (10 μL) was added and the mixture stirred at room temperature for 48 h. PLGA-Dextran (PD) was obtained by precipitation in methanol/diethyl ether (50/50 v/v), washed three times by methanol/diethyl ether and water by three times, and finally dried by lyophilization. Yield: 0.17 g (77%). ^{1}H NMR (DMSO − d_6, 400 MHz): 5.21 ppm (m, -OCH(CH_3)CONH-), 4.91 (m, -OCH_2COO-), 3.20–3.74 ppm (m, dextran glucosidic protons), 4.67 ppm (s, dextran hydroxyl protons), 4.49 ppm (s, dextran anomeric proton), 1.48 (d, -OCH(CH_3)CONH-) ppm.

2.3.2. Synthesis of PLGA-Dextran-Cy5.5 (PD-Cy5.5)

PLGA-Dextran-Cy5.5 was synthesized from PD and sulfo-Cyanine5.5 NHS ester as depicted in Scheme 2. Sulfo-Cyanine5.5 NHS ester (5 mg) and PD (50 mg) were dissolved in 4 mL dry DMSO followed by addition of DIPEA (8 μL). The reaction was stirred at room temperature for 48 h. PD-Cy5.5 was obtained by dialysis against water (MWCO 10 kDa) followed by lyophilization.

2.3.3. Synthesis of PLGA-PEG-Mannose (PPM) (Scheme 3)

tBOC-NH-PEG-Mannose. tBOC-NH-PEG-NHS (0.2 g, 0.06 mmol) and MAN (0.0195 g, 0.072 mmol) were dissolved in dry DMF (1 mL) followed by addition of DIPEA (103 μL, 0.6 mmol). The solution was stirred at room temperature for 48 h. tBOC-NH-PEG-Mannose was obtained by precipitation in diethyl ether, further washed by diethyl ether for two times and vacuum dried. Yield: 0.205 g (95%). ^{1}H NMR (DMSO, 400 MHz): 7.5, 7.0 ppm (d, phenyl proton), 5.26–4.4 ppm (m, mannose proton), 3.5 ppm (s, -CH_2CH_2O-), 1.37 ppm (s, -C(CH_3)$_3$) (Fig. S4).

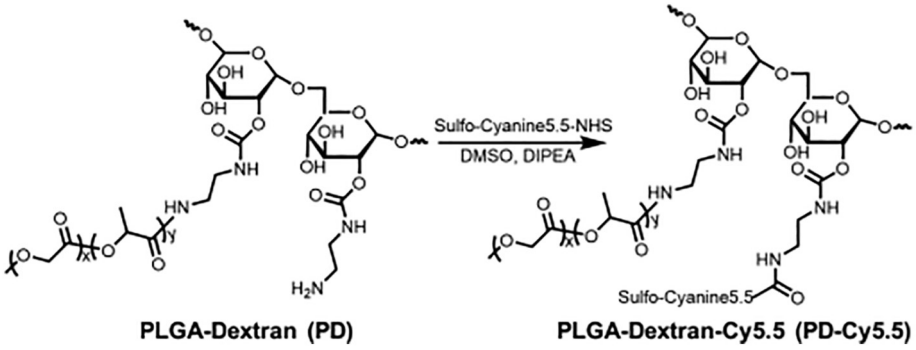

Scheme 2. Synthetic route of PLGA-Dextran-Cy5.5 (PD-Cy5.5).

NH_2-PEG-Mannose. tBOC-NH-PEG-Mannose (0.2 g) was dissolved in 4 mL DCM containing 50 vol% TFA and stirred at room temperature for 50 min. The reaction solvent was removed by rotary evaporation and the product was dialyzed against water (MW = 1 kDa) for three days. Finally, NH_2-PEG-Mannose was obtained by lyophilization. Yield: 0.15 g (75%). ^{1}H NMR (DMSO, 400 MHz): 7.5, 7.0 ppm (d, phenyl proton), 5.26–4.4 ppm (m, mannose proton), 3.5 ppm (s, -CH_2CH_2O-) (Fig. S6).

PLGA-PEG-Mannose (PPM). PLGA (0.2 g) was dissolved into dry DCM (1.5 mL). EDC·HCl (10 mg, 0.05 mmol) dissolved by 0.5 mL dry DCM and NHS (5.7 mg, 0.05 mmol) dissolved by 10 μL DMSO were added in sequence. The solution was stirred at room temperature for 2 h. PLGA-NHS was obtained by precipitated in cold methanol/diethyl ether (50/50 v/v), further washed two times and dried by rotary evaporation. PLGA-NHS was dissolved in dry DCM (2 mL) and subsequently NH_2-PEG-Mannose (0.026 g) was dissolved into the solution. DIPEA (10 μL) was added and the mixture stirred at room temperature for 48 h. PLGA-PEG-Mannose (PPM) was obtained by precipitation in methanol/diethyl ether (50/50 v/v) and washed three times by methanol/diethyl ether and finally vacuum dried to remove the solvent. Yield: 0.19 g (87%). ^{1}H NMR (D_2O, 400 MHz): 7.5, 7.0 ppm (d, phenyl proton), 5.20 ppm (m, -OCH(CH_3)CONH-), 4.91 ppm (m, -OCH_2COO-), 3.51 ppm (s, -CH_2CH_2O-), 1.48 (d, -OCH(CH_3)CONH-) ppm.

2.3.4. Synthesis of PLGA-PEG-Galactose (PPG)

tBOC-NH-PEG-Galactose. tBOC-NH-PEG-NHS (0.2 g, 0.06 mmol) and GAL (0.0195 g, 0.072 mmol) were dissolved in dry DMF (1 mL) followed by addition of DIPEA (103 μL, 0.6 mmol). The solution was stirred at room temperature for 48 h. tBOC-NH-PEG-Galactose was obtained by precipitation in diethyl ether, further washed by diethyl ether for two times and vacuum dried. Yield: 0.205 g (95%). ^{1}H NMR (DMSO, 400 MHz): 7.48, 6.95 ppm (d, phenyl proton), 5.34–4.1 ppm (m, galactose proton), 3.49 ppm (s, -CH_2CH_2O-), 1.37 ppm (s, -C(CH_3)$_3$) (Fig. S5).

NH_2-PEG-Galactose. tBOC-NH-PEG-Galactose (0.2 g) was dissolved in 4 mL DCM containing 50 vol% TFA and stirred at room temperature for 50 min. The reaction solvent was removed by rotary evaporation and the product was dialyzed against water (MW = 1 kDa) for three days. Finally, NH_2-PEG-Galactose was obtained by lyophilization. Yield: 0.15 g (75%). ^{1}H NMR (DMSO, 400 MHz): 7.48, 6.95 ppm (d, phenyl proton), 5.34–4.1 ppm (m, galactose proton), 3.5 ppm (s, –CH_2CH_2O-).

PLGA-PEG-Galactose (PPG). The synthetic route was illustrated in Scheme 4. Briefly, PLGA (0.2 g) was dissolved into dry DCM (1.5 mL). EDC·HCl (10 mg, 0.05 mmol) dissolved by 0.5 mL dry DCM and NHS (5.7 mg, 0.05 mmol) dissolved by 10 μL DMSO were added in sequence. The solution was stirred at room temperature for 2 h. PLGA-NHS was obtained by precipitated in cold methanol/diethyl ether (50/50 v/v), further washed two times and dried by rotary evaporation. PLGA-NHS was dissolved in dry DCM (2 mL) and subsequently NH_2-PEG-Galactose (0.026 g) was dissolved into the solution. DIPEA (10 μL) was added and the mixture stirred at room temperature for 48 h. PLGA-PEG-Galactose (PPG) was obtained by precipitation in methanol/diethyl ether (50/50 v/v) and washed three times by methanol/diethyl ether and finally vacuum dried to remove the solvent. Yield: 0.19 g (87%). ^{1}H NMR (D_2O, 400 MHz): 7.51, 6.97 ppm (d, phenyl proton), 5.21 ppm (m, -OCH(CH_3)CONH-), 4.93 ppm (m, -OCH_2COO-), 3.53 ppm (s, -CH_2CH_2O-), 1.49 ppm (d, -OCH(CH_3)CONH-).

2.3.5. Synthesis of PLGA-PEG-Cy5.5 (PP-Cy5.5)

NH_2-PEG-Cy5.5. NH_2-PEG-Thiol (0.014 g, 0.06 mmol) and Sulfo-Cyanine5.5 maleimide (5 mg, 0.072 mmol) were dissolved in phosphate-buffered saline (PBS, pH =7.0, 2 mL) accompanied by N_2 purging. The solution was stirred and protected from light at room temperature for 48 h. NH_2-PEG-Cy5.5 was obtained by dialyzing against water (MW = 2 kDa) until the dialysate has no absorption at 673 nm. Finally, NH_2-PEG-Cy5.5 was obtained by lyophilization. Yield: 0.018 g (99%).

PLGA-PEG-Cy5.5 (PP-Cy5.5). The synthetic route was illustrated in

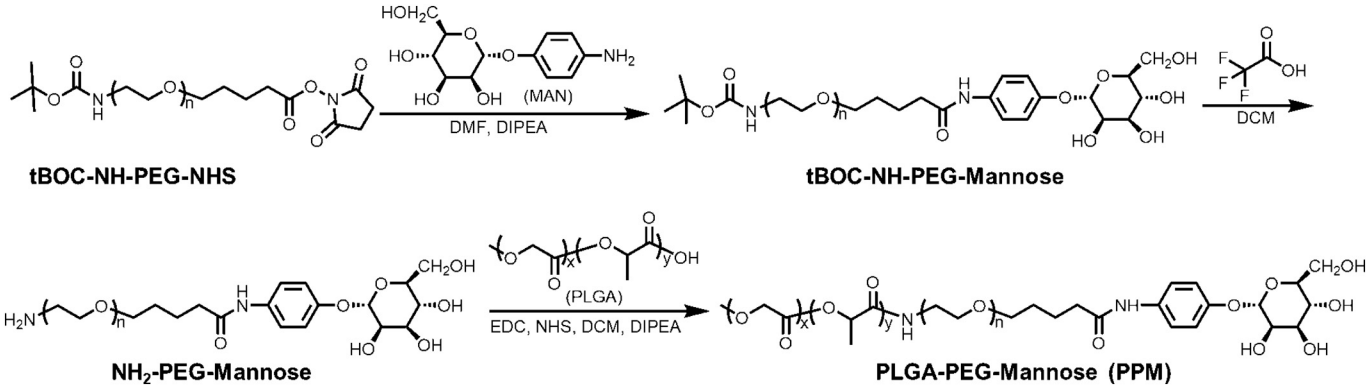

Scheme 3. Synthetic route of PLGA-PEG-Mannose (PPM).

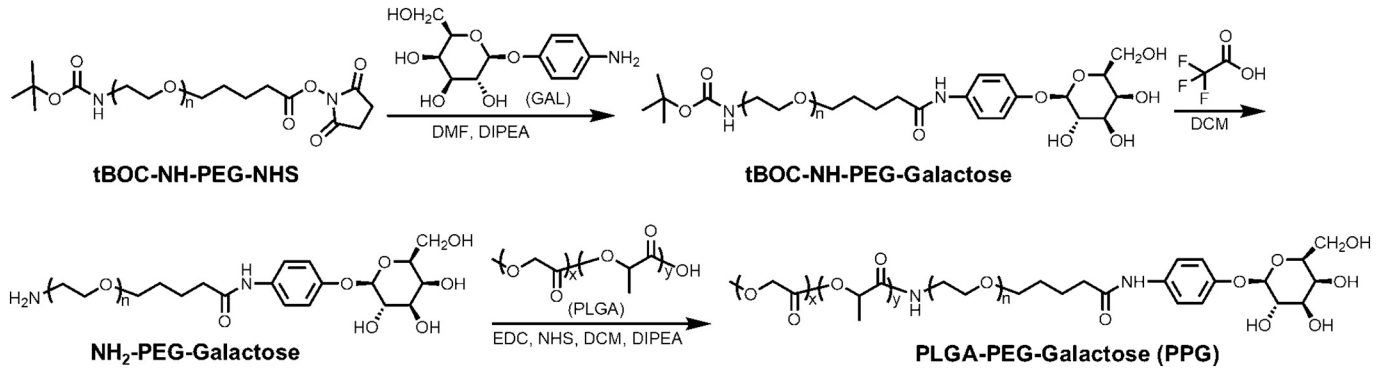

Scheme 4. Synthetic route of PLGA-PEG-Galactose (PPG).

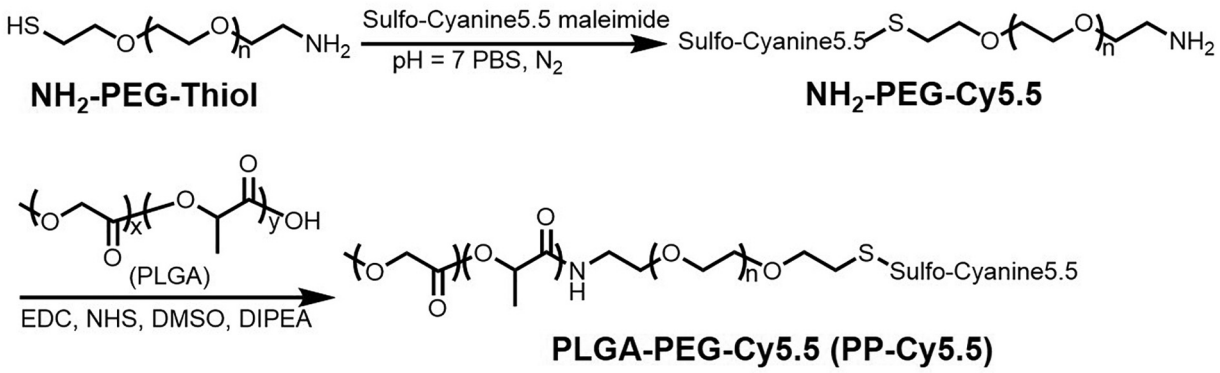

Scheme 5. Synthetic route of PLGA-PEG-Cy5.5 (PP-Cy5.5).

Scheme 5. Briefly, PLGA (0.132 g) was dissolved into dry DCM (1.5 mL). EDC·HCl (6 mg, 0.03 mmol) dissolved by 0.5 mL dry DCM and NHS (3.7 mg, 0.03 mmol) dissolved by 10 μL DMSO were added in sequence. The solution was stirred at room temperature for 2 h. PLGA-NHS was obtained by precipitated in cold methanol/diethyl ether (50/50 v/v), further washed two times and dried by rotary evaporation. PLGA-NHS was dissolved in dry DCM (2 mL) and subsequently NH_2-PEG-Cy5.5 (0.018 g) was dissolved into the solution. DIPEA (7 μL) was added and the mixture stirred at room temperature for 48 h. PLGA-PEG-Cy5.5 (PP-Cy5.5) was obtained by precipitation in methanol/diethyl ether (50/50 v/v) and washed three times by methanol/diethyl ether and finally vacuum dried to remove the solvent. Yield: 0.106 g (72%).

2.3.6. Synthesis of PLGA-PEG (PP)

The synthesis route of PP was depicted in Scheme 6. PLGA (0.2 g, 5 μmol) was dissolved into dry DCM (1.5 mL). EDC·HCl (10 mg, 0.05 mmol) dissolved by 0.5 mL dry DCM and NHS (5.7 mg, 0.05 mmol) dissolved by 10 μL DMSO were added in sequence. The solution was stirred at room temperature for 2 h. PLGA-NHS was obtained by precipitated in cold methanol/diethyl ether (50/50 v/v), further washed two times and dried by rotary evaporation. PLGA-NHS was dissolved in dry DCM (2 mL) and subsequently NH_2-PEG-OH (0.018 g, 6 μmol) was dissolved into the solution. DIPEA (10 μL) was added and the mixture stirred at room temperature for 24 h. PP was obtained by precipitation in methanol/diethyl ether (50/50 v/v) and washed three times by methanol/diethyl ether and finally vacuum dried to remove the solvent. Yield: 0.2 g (90%). ^{1}H NMR ($CDCl_3$, 400 MHz): 5.21 ppm (m, -O*CH*(CH_3)CONH-), 4.82 ppm (m, -O*CH*$_2$COO-), 3.64 ppm (s, -*CH*$_2$*CH*$_2$O-), 1.57 (d, -OCH(*CH*$_3$)CONH-) ppm.

2.3.7. Synthesis of cationic lipid compound (G0-C14)

The cationic lipid-like compound G0-C14 was synthesized from PAMAM dendrimer G0 using a ring-opening reaction by reacting with 1,2 epoxytetradecane according to previously described procedures [28]. Briefly, 1,2 epoxytetradecane was mixed with PAMAM dendrimer G0 at a molar ratio of 5:1, whereby substoichiometric amounts of 1,2 epoxytetradecane were added to increase the proportion of products with three less tail than the total possible for a given amine monomer. The mixture was reacted under vigorous stirring at 90 °C for 2 d.

2.3.8. NP preparation

All of the NPs preparation was conducted by a nanoprecipitation method and the PPM NPs preparation was as follows. PPM material of 5 mg containing 10% (mass fraction) PP-Cy5.5 was dissolved into DMSO (1 mL) and added dropwise to PVA aqueous solution (10 mL, 0.1% w/v) which was stirred at 500 rpm. After the dropping, the mixture was continuously stirred for 30 min. Then the mixture was transferred into an Amicon Ultra-4 centrifugal filter (Millipore, Billerica, MA) with a molecular weight cutoff of 100 kDa and washed three times to remove the organic solvent and free molecules. The NPs were diluted 20-fold in water for size determination using DLS. PP-Cy5.5 was used to dope with PP to prepare fluorescently-labeled NPs that contain the polymer PP. PD-Cy5.5 was used to dope with PD to produce fluorescently-labeled PD NPs.

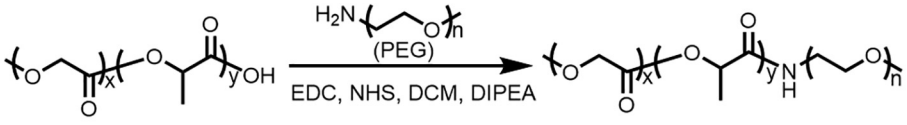

Scheme 6. Synthetic route of PLGA-PEG (PP).

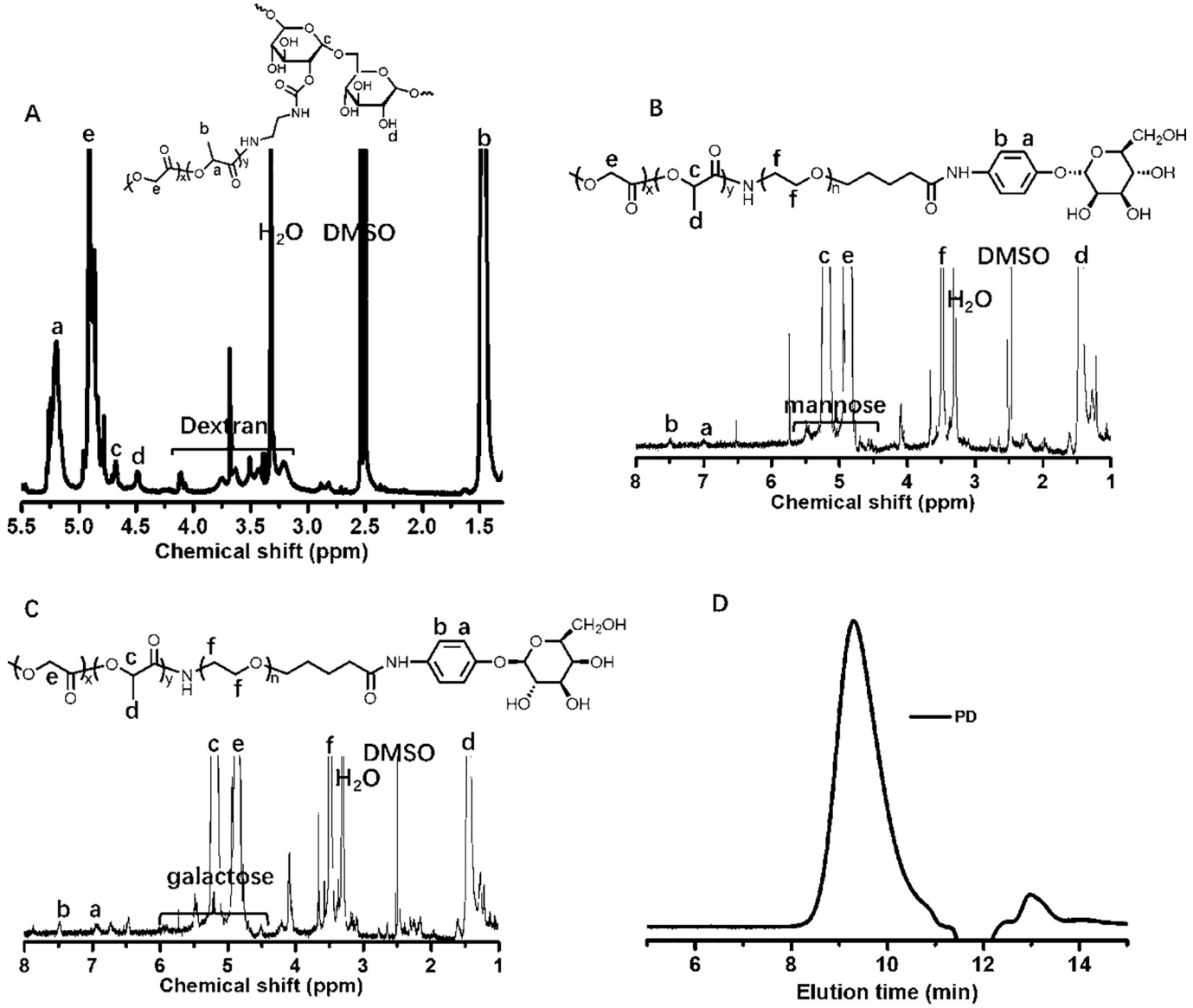

Fig. 1. ^{1}H NMR spectra characterization of (A) PD, (B) PPM and (C) PPG polymers in DMSO-d_6. (D) GPC traces of PD polymer.

2.3.9. Macrophage cell culture and analysis of NPs uptake

RAW 264.7 cells were cultured in DMEM supplemented with 10% FBS and 1% penicillin/streptomycin (P/S) at 37 °C in a humidified 5% CO_2-containing atmosphere. Then NPs doped with fluorescent dye (*i.e.* PD-Cy5.5 or PP-Cy5.5) at the concentration of 0, 0.45, 0.9, 1.6 and 2.8 mg/mL were added into the wells and the cells were incubated for 4 h. Afterward, the medium was replaced by fresh complete medium. After further cultured for 12 h, the cells were washed with PBS 3 times and blowed from the plate. Cells suspended in PBS were analyzed *via* flow cytometry to assess cellular uptake of NPs.

2.3.10. Cytotoxicity of NPs

To perform the NPs cytotoxicity test, Raw 264.7 cells were seed in 96-well cell culture plates at the density of 1×10^4 cells/well for 24 h. NP dispersions were diluted with PBS and then added to the well at the concentration of 0, 0.9, 1.6 and 2.8 mg/mL, respectively. After incubated for another 24 h, the cell viability was analyzed by CCK-8 assay. Briefly, the medium was removed and the wells were washed twice with PBS. Ten microliters of CCK-8 solution were added to each well of the plate and incubated for 2 h. The absorbance at 450 nm was measured using a microplate reader.

2.3.11. Nucleic acid complexation ability of G0-C14 and its stability in organic solvent

To assess the nucleic acid complexation ability of G0-C14 and its stability in organic solvent (DMF), naked nucleic acid or nucleic acid complexed with G0-C14 (in varying weight ratios from 0.1 to 40) were incubated with or without DMF for 10 min. For nucleic acid samples in DMF, electrophoresis was run without extracting nucleic acid from DMF into aqueous solution. The volumes of samples were then adjusted with loading dye and run into an *E*-Gel 1% agarose (Invitrogen) gel for 20 min at 100 V. The Ambion Millennium markers-Formamide (Thermo Fisher Scientific) was used as a ladder. Finally, the gel was imaged under ultraviolet and the bands were analyzed.

2.3.12. Preparation of nucleic acid NPs

We employed a robust, self-assembly method to prepare nucleic acid (GFP DNA or EGFP mRNA) encapsulated polymer–lipid hybrid NPs. PP, PPM, PD and G0-C14 were dissolved separately in DMF at concentrations of 2 mg ml^{-1}, respectively. The preparation of PP NPs without targeting moieties was as follows. PP (300 μg in 150 μL) and G0-C14 (300 μg in 150 μL) were mixed at a weight ratio of 1:1 in a small glass vial. Nucleic acid (10 μg at 1 mg/mL concentration) in aqueous solution

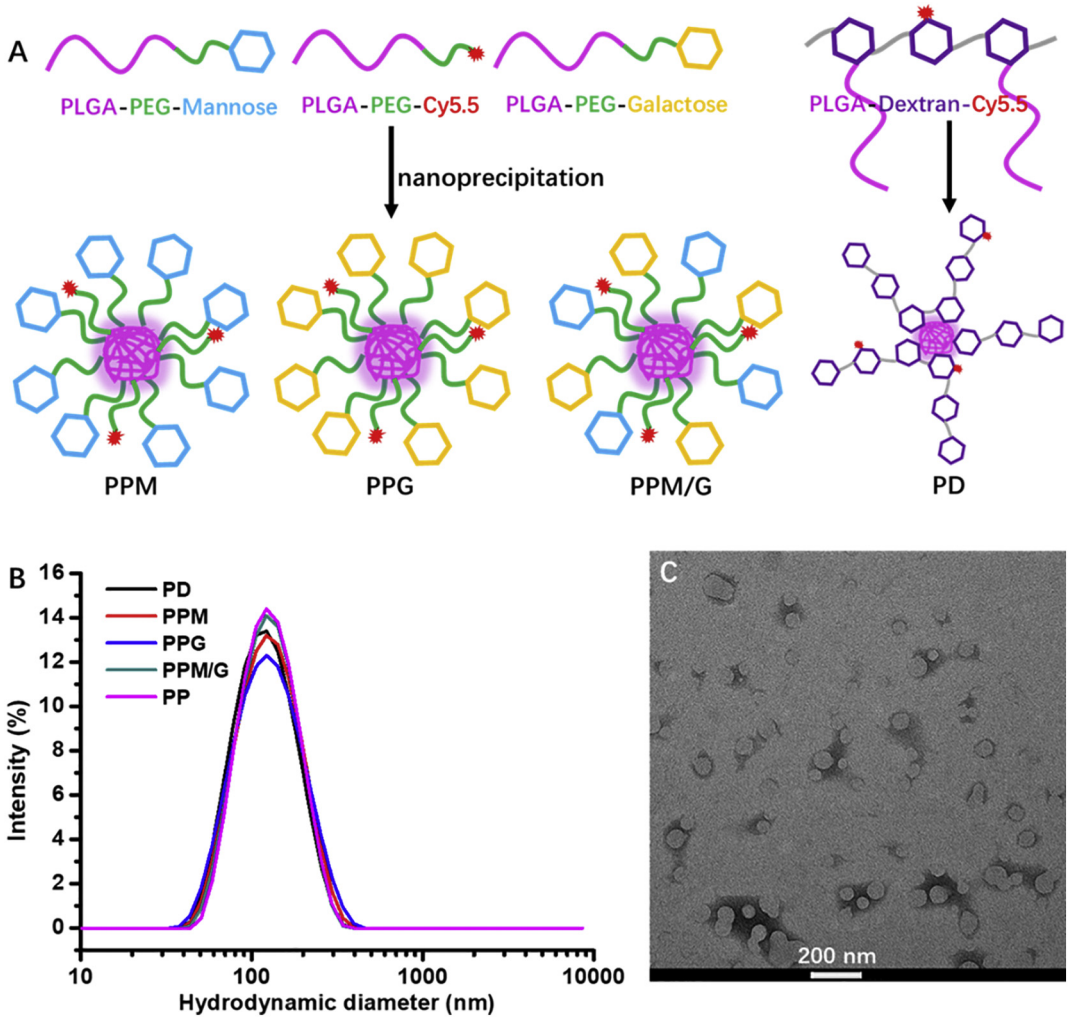

Fig. 2. (A) Schematic diagram of macrophage-targeted NPs decorated with different carbohydrates. (B) Hydrodynamic diameters of NPs prepared by a nanoprecipitation method. (C) TEM image of PPM NPs stained with 1% uranyl acetate.

was mixed into the PP/G0-C14 organic solution (weight ratio of nucleic acid:PP:G0-C14 was 1:30:30) to form cationic lipid/nucleic acid nanocomplexes. This solution was then precipitated drop by drop into 10 mL of PVA aqueous solution (2.5 mg ml^{-1} concentration in DNase/RNase-free Hypure water). Upon nanoprecipitation, NPs formed instantly and were kept stirring for 20 min at 500 rpm to stabilize. The NPs were then washed three times with ice-cold Hypure water using Amicon tubes (molecular weight cut-off, 100 kDa; Millipore) to remove organic solvent and free compounds and finally concentrated into 1 mL PBS solution. The NPs were used fresh or kept at −80 °C to use later for various *in vitro* studies. The NPs loading with mRNA or pDNA were subjected to gel electrophoresis as described above to check for any leaching of unencapsulated nucleic acid. According to the above formulation, PP was replaced partially or completely by PPM or PD to obtain NPs with targeting moieties and the detailed information was listed in Tables S1 & S2.

2.3.13. Release of mRNA from the NPs

To analyze the release profile of NPs, Cy5-labeled EGFP mRNA (5-moUTP, APExBIO Technology LLC, Texas) was first encapsulated into the NPs. A suspension of NPs in PBS was aliquoted (100 μL) into several semipermeable minidialysis tubes (molecular mass cutoff of 100 kDa; Pierce) and dialyzed against 2 L of frequently renewed PBS (pH 7.4) at 37 °C with gentle stirring. At predetermined time points, quintuplicate aliquots of each NP sample (n = 5) were withdrawn, and a standard curve correlating fluorescence and Cy5 mRNA concentration was used to determine the amount of mRNA encapsulated within the NPs. The fluorescence intensity was measured by a multimode microplate reader (excitation/emission 650/670 nm; TECAN, Inc.). The amounts of released mRNA were calculated to generate a cumulative release curve.

2.3.14. Cell culture

RAW 264.7 cell line purchased from American Type Culture Collection (ATCC) was used for *in vitro* studies. The cells were maintained in DMEM cell culture medium, supplemented with 10% fetal bovine serum inactivated at 56 °C for 30 min and 1% penicillin-streptomycin antibiotic. Cell culture and all biological experiments were performed at 37 °C in 5% CO_2 conditions in a cell culture incubator.

2.3.15. In vitro transfection activity of nucleic acid NPs

Raw 264.7 Cells were seeded on a 24-well plate at a density of 1×10^5 cells per well and allowed to attach and grow in 24 h. Cells were transfected with nucleic acid NPs at various nucleic acid concentrations (0.125, 0.250, 0.500 and 1.000 μg/mL) for 4 h in DMEM followed by replacement with fresh complete medium and further incubated for 24 h to check transfection efficiency. For transfection efficiency measurement, cells were collected and washed twice and resuspended in PBS followed by measuring GFP expression using flow cytometry. The data were analyzed using Flowjo software and expressed as both percentages of GFP-positive cells and mean

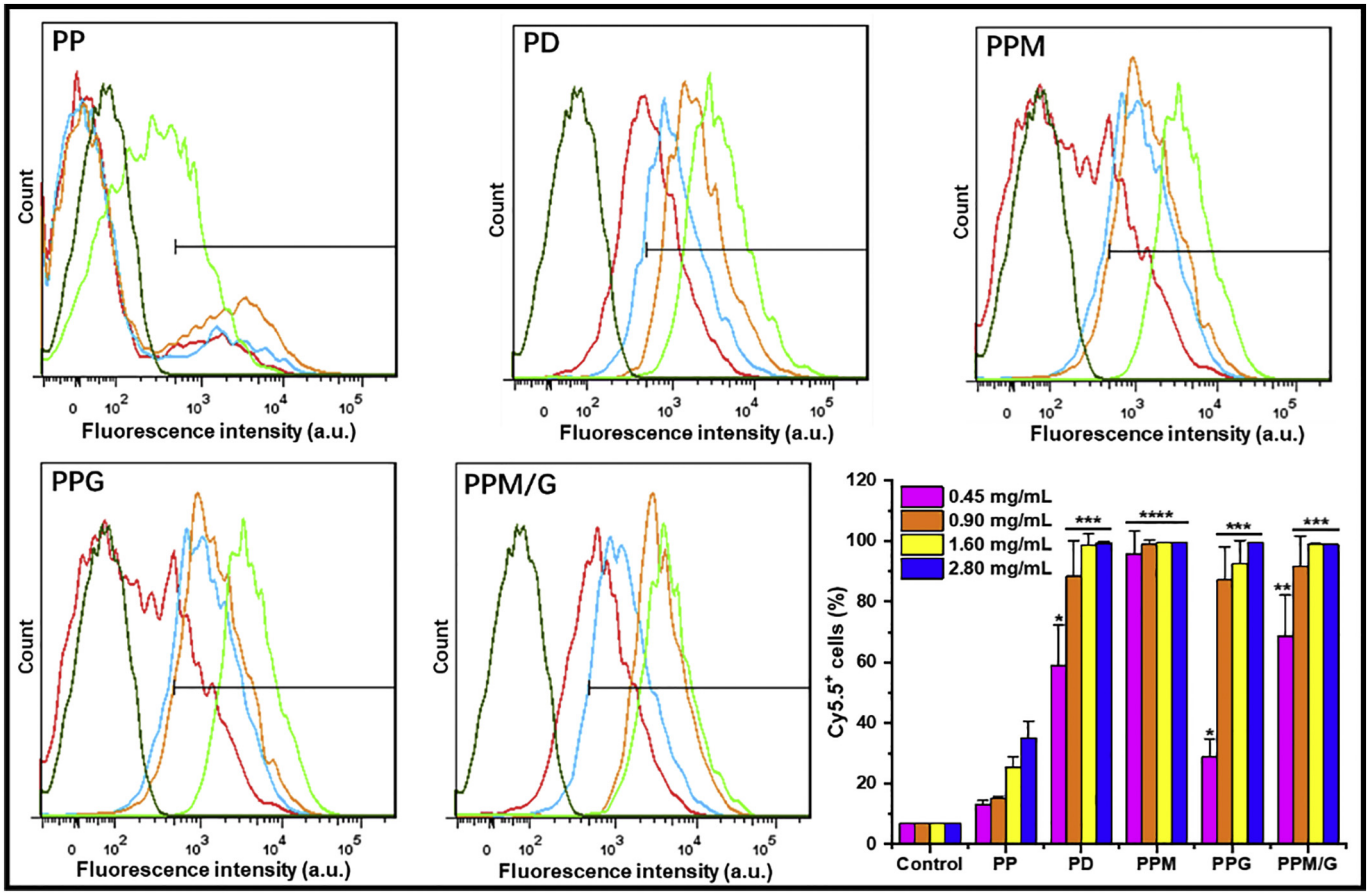

Fig. 3. Cellular uptake of NPs by Raw 264.7 cells after incubation with various NPs at different concentrations of 0 mg/mL (control group, indicated by the black curve for each histogram), 0.45 mg/mL (red curves), 0.90 mg/mL (blue curves), 1.60 mg/mL (orange curves), 2.80 mg/mL (green curves), and the bar graph showing the corresponding endocytosis efficiency (percentage of Cy5.5-positive cells). The statistical significance is calculated by Student's *t*-test, and represents the comparison between targeted NPs with the untargeted PP NPs at each concentration ($^{*}P < .05$, $^{**}P < .01$, $^{***}P < .001$ and $^{****}P < .0001$). Data are presented as the mean ± standard deviation (n = 3). (For interpretation of the references to colour in this figure legend, the reader is referred to the web version of this article.)

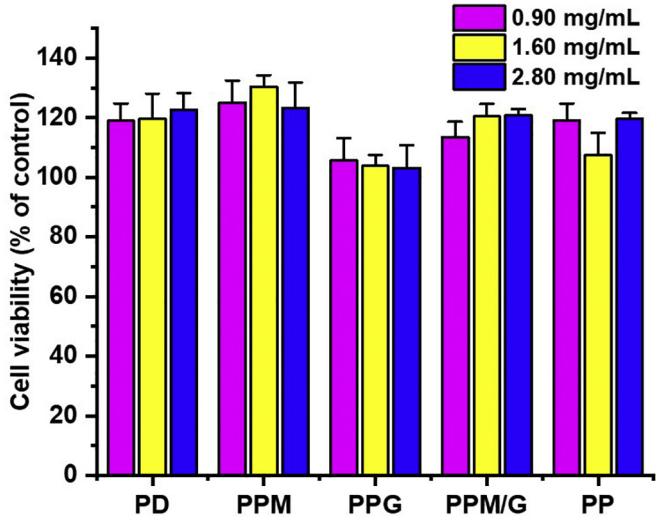

Fig. 4. Cytotoxicity of various NPs against Raw 264.7 cells at different concentrations of 0.90 mg/mL, 1.60 mg/mL, and 2.80 mg/mL. Cell viability was normalized to the untreated control group. Data are presented as the mean ± standard deviation (n = 5).

fluorescence intensity (MFI).

2.3.16. Statistical analysis

Data are expressed as the mean ± standard deviationn (SD). Statistical analysis was carried out using GraphPad Prism 8.0 software to perform two-sided *t*-tests. A *P* value less than 0.05 was considered statistically significant.

3. Results and discussion

3.1. Synthesis and characterization of carbohydrate-conjugated PLGA or PLGA-PEG polymers

As shown in Fig. 1A, peak c (4.49 ppm, dextran anomeric proton) and peak a (5.21 ppm, –O*CH*(CH_3)CONH-) in ^{1}H NMR spectrum of PD were used to evaluate the number of PLGA chains per dextran. The number of PLGA chains grafted to dextran can be controlled by adjusting the feeding molar ratio (γ), and the grafted PLGA chains had an average number of 20 per dextran when γ of PLGA/D-70-NH_2 was 18.4. The GPC traces of PD showed that there was no unreacted PLGA left and the polymer had a low polydispersity ($Đ < 1.2$) (Fig. 1D). The synthetic methods of PPM and PPG polymers were similar and successively passed through acylation, deprotection of amine, and acylation reactions(Scheme 3 & 4). In the first step, the reaction ratio of mannose or galactose grafting to PEG was 100%, which was obtain by calculating the integral peak areas between the phenyl proton (7.5, 7.0 ppm) and the tert-butyl proton in Boc (tert-butyloxycarbonyl) group (1.37 ppm,

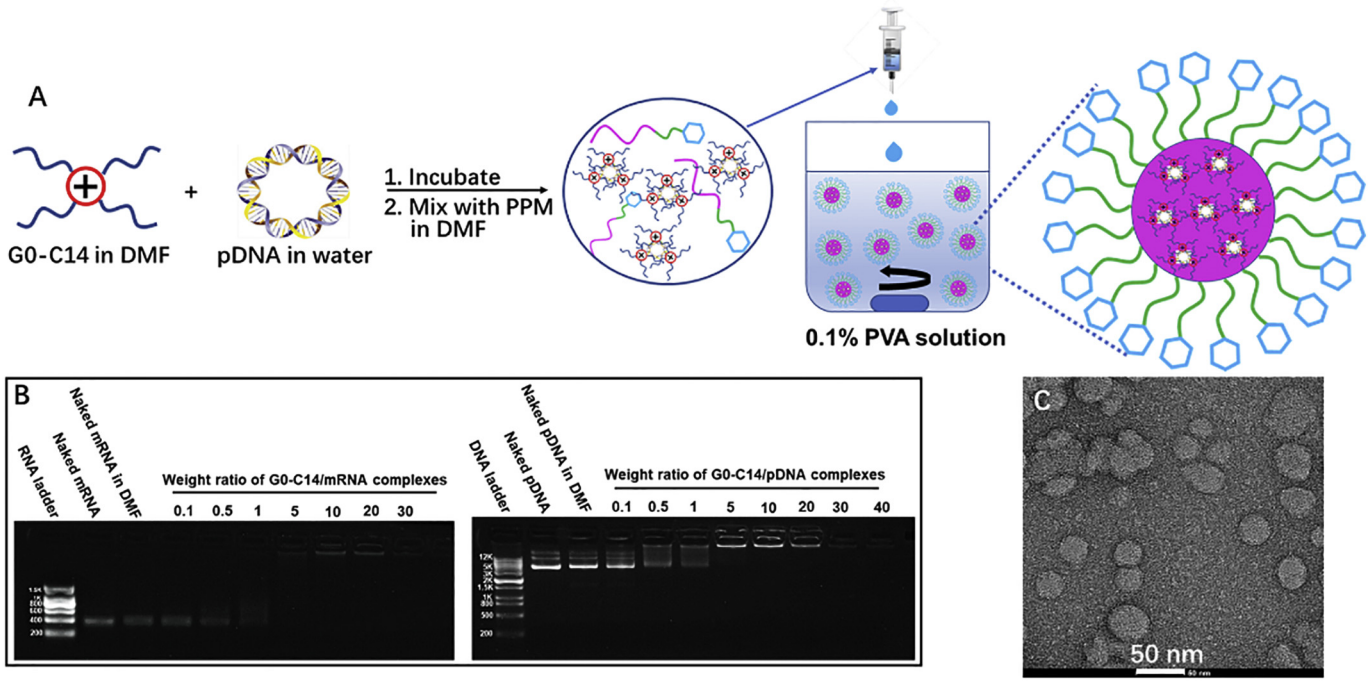

Fig. 5. (A) Schematic representation of the self-assembly process of pDNA-loaded PPM/G0-C14 hybrid NPs. (B) Electrophoretic analysis of mRNA and pDNA mobility in the complexes with G0-C14. (C) TEM image of pDNA-loaded PPM/G0-C14 NPs stained with 1% uranyl acetate.

-C(CH_3)$_3$) (Fig. S4&S5). In the second step, the Boc group was completely removed due to the disappearance of the peak at 1.37 ppm (Fig. S6). At last, PPM and PPG were further prepared by acylation reaction with PLGA and the ^{1}H NMR spectra were presented in Fig. 1B and C, respectively. All the reaction rates were above 80% by calculating integral areas of peak f and d.

3.2. Preparation and characterization of NPs

We used carbohydrate-decorated polymers to design and prepare a series of NPs by nanoprecipitation techniques (Fig. 2A). In brief, the polymer was dissolved into an organic solvent and added dropwise into the deionized water. Two kinds of NPs were formulated including NPs of the same composition (*i.e.* PPM, PPG and PD) and PPM/G NP constructed from a mixture of PPM and PPG at weight ratio of 1:1. Moreover, in the formulation process, Cy5.5-labeled PLGA-PEG (PP-Cy5.5) was incorporated into the NPs for the subsequent flow cytometry characterization of phagocytosis of NPs by macrophages. The average hydrodynamic size of the yielded NPs was measured using dynamic-light scattering (DLS). We found that the particle size was dependent on the type of organic solvent used and the polymer concentration. The particle size was bigger when acetone was used for NP formulation compared to that of DMSO, also an increase in polymer concentration resulted in an increase in particle size. Moreover, the size of PD NP was also dependent on the number of PLGA chains grafting to dextran. PLGA chains grafted to dextran with an average number of 10, 20 and 33 gave a corresponding average PD NP size of 85 nm, 147 nm and 263 nm, respectively. The particle size gradually increased with the incorporation of PLGA which constituted the hydrophobic central core of the NP. Herein, PD with 20 PLGA chains per dextran was used for NP preparation to achieve a uniform size for all NPs (Fig. 2B). The size of all the NPs was found to be 136 ± 10.9 nm (mean ± SD) with a polydispersity index (PDI) ≤ 0.2. TEM image of PPM NPs stained with uranyl acetate showed a monodisperse and spherical morphology, with a particle size less than that of DLS due to syneresis (Fig. 2C).

3.3. NPs uptake by macrophages

To investigate the impact of carbohydrate type on the macrophage-targeting capability of NPs, Cy5.5 was added during the self-assembly process to prepare fluorescently-labeled NPs with various carbohydrate moieties. These fluorescently-labeled NPs were then incubated with RAW 264.7 macrophages for different time periods at given concentrations. Cells without NP treatment were used as a control group. Cy5.5-positive cells were then detected using flow cytometry to investigate the impact of carbohydrate type on the macrophage-targeting capability of NPs. As shown in the histogram (Fig. 3), the fluorescence peaks shifted right compared with the control group if more cells uptake the fluorescently-labeled NPs. Treatment with PP NPs without carbohydrate moieties at the maximum concentration of 2.8 mg/mL resulted in only 34% of Cy5.5-positive cells. Note that NPs with carbohydrate moieties, particularly PD NPs and PPM NPs, showed significantly higher endocytosis efficiency than non-targeted PP NPs even at a low concentration of 0.45 mg/mL, indicating that incorporation of dextran or mannose moiety could facilitate the receptor-mediated internalization of NPs (Fig. 3). Partial replacement of PPM with PPG led to reduced cellular uptake of NPs. The Cy5.5-positive signal remarkably increased with the increasing concentration of carbohydrate-decorated NPs, and attained to above 90% with a concentration of 1.6 mg/mL or above. NPs decorated with dextran or mannose moiety were used in the following *in vitro* transfection experiments.

3.4. In vitro cell viability of NPs

A promising nonviral vector should achieve both sufficient transfection efficiency and low cytotoxicity. The developed NPs were synthesized using carbohydrate-modified PLGA or PLGA-PEG which are biocompatible, biodegradable and safely administrable polymers approved by the US FDA (Food and Drug Administration) and EMA (European Medicines Agency). *In vitro* cytotoxicity of the different NPs was evaluated in Raw 264.7 cells at various concentrations by CCK-8 assay (Fig. 4). The data showed that cell viability was not discernibly affected by either non-targeted PP NPs or carbohydrate-decorated NPs

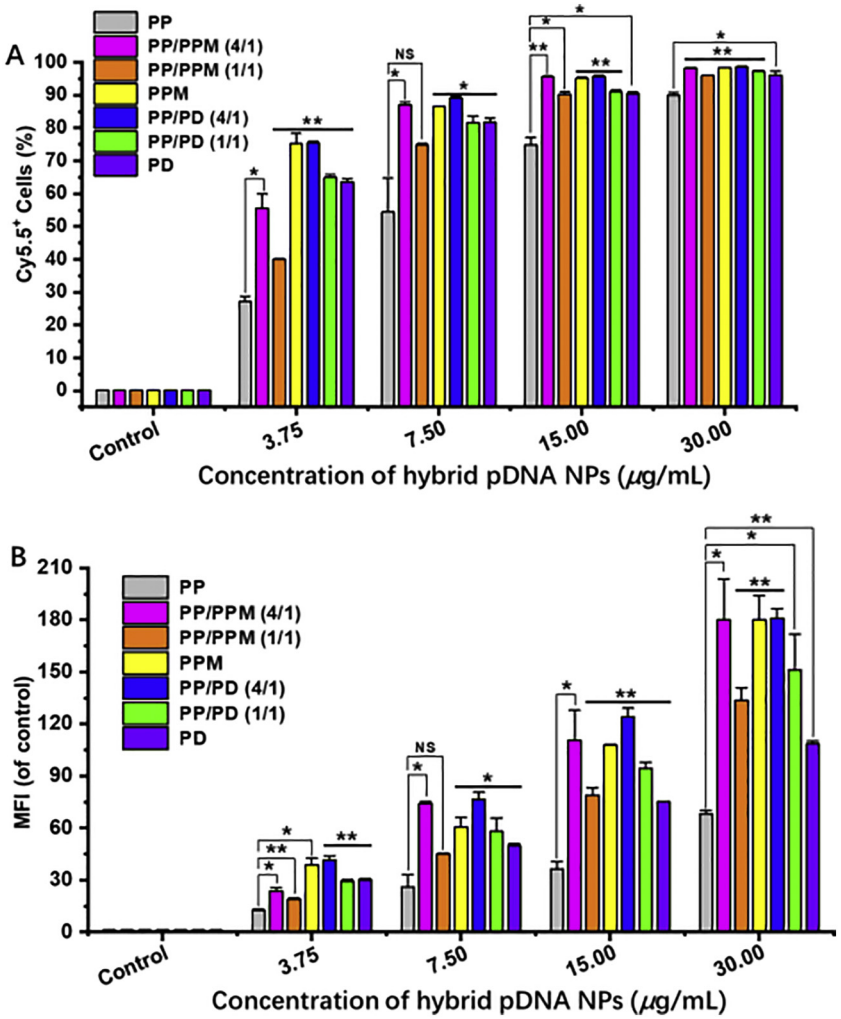

Fig. 6. Phagocytosis efficiency of the different NPs at various concentrations in macrophages. The data were expressed as a percentage (A) and MFI (B) of Cy5.5-positive ($Cy5.5^+$) cells. MFI of Cy5.5 was calculated using Flowjo software and normalized to the untreated control group. Data are presented as the mean ± standard deviation (n = 3), and the statistical significance determined by Student's *t*-test represents the comparison between targeted NPs with the untargeted PP NPs. $^{***}P < .001$, $^{**}P < .01$, $^{*}P < .05$. NS refers to not significant.

at a very high NP concentration of 2.8 mg/mL which is much higher than the concentration required for gene transfection. These results indicate that both the PP NP and the tested carbohydrate-decorated NPs might serve as safe carriers for gene delivery *in vivo*.

3.5. In vitro transfection activity

The hybrid NPs were prepared by nanoprecipitation method using the cationic lipid-like compound G0-C14 and carbohydrate-decorated PLGA or PLGA-PEG polymers. Fig. 5A presents the preparation process of pDNA-loaded PPM/G0-C14 NPs as an example. G0-C14 was used for gene complexation and polymer was used to make a stable NP core. Moreover, the polymer/G0-C14 layer can protect and entrap the nucleic acid payload within the NP to control gene release. Cy5-labeled EGFP mRNA was first encapsulated into the NPs, and the amounts of encapsulated mRNA were determined based on fluorescence measurement using standard curves of Cy5 mRNA. The result showed that PPM/G0-C14 NPs were able to encapsulate more than 95% of the initial mRNA. To measure mRNA release kinetics, Cy5 mRNA-loaded PPM/G0-C14 NP samples were dialyzed against 2 L of frequently renewed PBS (pH 7.4) at 37 °C to mimic physiological conditions. The release profile of Cy5 mRNA was measured using fluorescent spectrophotometry, which indicated that around 50% of the total mRNA was released from the NPs over the first 30 h and then reached a maximum value of 89% over 8 d (Fig. S7). The above results demonstrated that the synthesized polymer/G0-C14 NPs enabled the dense loading and sustained release of nucleic acids.

The ability of G0-C14 vectors to condense mRNA and pDNA was evaluated by an electrophoresis retardation assay at different weight ratios. EGFP mRNA and GFP pDNA were used as the model mRNA and pDNA to evaluate the gene complexation ability of G0-C14. As shown in Fig. 5B, the intensity of the migrating free mRNA or pDNA bands decreased gradually with an increase in weight ratio (from 0.1/1 to 30/1 or 0.1/1 to 40/1, respectively), indicating a strong gene compaction capability of G0-C14. G0-C14 effectively condensed EGFP mRNA and GFP pDNA, leading to a complete retardation of mRNA and pDNA at a weight ratio of 5 or above. In order to obtain high encapsulation efficiency after multiple times washing during NP preparation process, the weight ratio of 30 was chosen to formulate NPs for the following *in vitro* transfection experiments.

We doped carbohydrate-decorated polymers (PPM or PD) into PP at different proportions to complete replacement of PP to prepare gene-loaded NPs with gradient targeting moieties. For example, PP/PPM (4/1) NPs were constructed using the mixture of PP and PPM polymers at a 4/1 mass ratio. The tested NPs were around 200 nm in hydrodynamic size with a narrow distribution as characterized by DLS (Table S1&S2). The average NP surface charge was near neutral (0 ± 0.57 mV) because the NPs have an outer lipid-PEG-mannose or lipid-dextran shell.

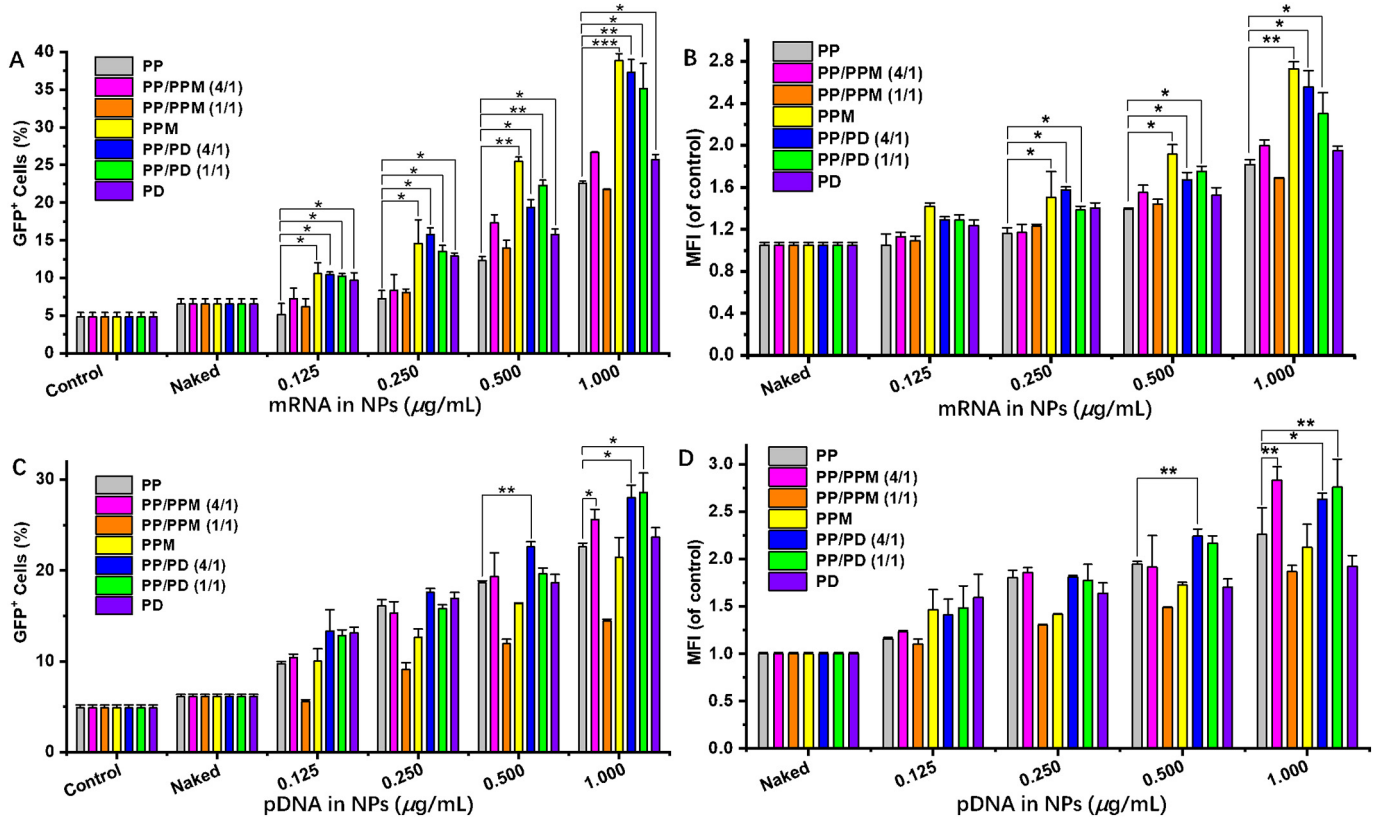

Fig. 7. Transfection efficiency in Raw 264.7 cells mediated by mRNA-loaded hybrid NPs (A & B) and pDNA-loaded hybrid NPs (C & D) at different gene concentrations of 0.125, 0.250, 0.500, and 1.000 μg/mL. The data were expressed as the percentage of GFP-positive cells (A & C) and MFI of GFP (B & D). MFI of GFP was calculated using Flowjo software and normalized to the control group (untreated cells). Data are presented as the mean ± standard deviation (n = 3), and statistical significance was calculated by Student's *t*-test: ***P < .001, **P < .01, *P < .05.

The NPs were found to be intact and spherical as characterized by transmission electron microscopy (TEM), with a post-dehydration size of ~50 nm (Fig. 5C). We also studied the stability of the NPs using PP/PPM (4/1) NP as an example, and found that there was no significant change in size and zeta potential following incubation at 37 °C for 24 h (Table S3).

To further investigate the impact of sugar content on the macrophage-targeting capability of NPs, Cy5.5-labeled PP or PD polymer (PP-Cy5.5 or PD-Cy5.5) was incorporated into the formulation process to prepare fluorescently-labeled NPs with different contents of mannose or dextran moiety as described above. Binding and uptake of the yielded carbohydrate-decorated NPs and non-targeted PP NPs within RAW 264.7 macrophages were quantitatively evaluated by detecting both Cy5.5-positive cells and MFI using flow cytometry. As shown in Fig. 6, the yielded NPs exhibited a strong cellular internalization in macrophages, which increased in a dose-dependent manner. Treatment with carbohydrate-decorated NPs at doses ranging from 3.75 μg/mL to 15 μg/mL resulted in a significantly higher percentage of Cy5.5-positive cells compared with non-targeted PP NPs (Fig. 6A). At a higher NP dose of 30 μg/mL or above, the enhancement effect was moderate since the percentage of Cy5.5-positive cells attained to above 90%. The MFI data demonstrated that carbohydrate-decorated NPs, particularly PP/PPM (4/1) NPs, PPM NPs and PP/PD(4/1) NPs, mediated significantly higher phagocytosis efficiency than non-targeted PP NPs at all tested doses (Fig. 6B). However, higher PD content in NPs led to lowered fluorescence intensity, indicating that there is an optimal carbohydrate density for PD-decorated NPs to promote specific interactions with macrophages.

We then evaluated the *in vitro* gene transfection efficacy of the NPs decorated with different contents of mannose or dextran moiety in Raw 264.7 cells using EGFP mRNA and GFP pDNA as reporter genes. NPs encapsulating both EGFP mRNA and GFP pDNA mediated highly efficient transfection in Raw 264.7 cells, which showed a dose-dependent increase in GFP expression that correlated with increasing gene concentrations (from 0.125 to 1.0 μg/mL) (Fig. 7). It is important to note that targeted PPM and PP/PD NPs mediated significantly higher mRNA transfection efficiency at various concentrations compared with non-targeted NPs (Fig. 7A and B). This was consistent with the above studies that PPM NPs and PP/PD(4/1) NPs showed remarkably high endocytosis efficiency. However, there was no obvious correlation between endocytosis efficiency and pDNA transfection efficiency of PPM and PP/PD NPs at concentrations of 0.125 μg/mL and 0.250 μg/mL (Fig. 7C and D). This is likely due to the way the gene is expressed. Gene-loaded hybrid NPs are first phagocytosed by the macrophages. Once NPs escape from the lysosome and release the gene payload into the cytoplasm, the message coded by the released mRNA is then translated into the target protein, but pDNA needs to further enter the nucleus and be transcribed in order for protein expression. In addition to cellular internalization, nuclear entry would be another barrier that must be overcome for successful pDNA delivery.

4. Conclusions

Macrophages play a critical role in the pathological processes of many diseases including diabetes, obesity, cancer, pulmonary fibrosis, cardiovascular diseases, and other inflammatory diseases. Macrophage-targeted gene therapy holds great promise as an alternative approach for reversing the underlying pathological damage at the site of inflammation, and therefore there is a major need for targeted gene carriers capable of safe and efficient delivery of therapeutic genes to macrophages in the inflammatory microenvironment. In this study, we demonstrate the development and investigated the efficacy of

controlled-release NPs decorated with different carbohydrates for targeted gene delivery to macrophages. The results showed that incorporation of the carbohydrate moieties, particularly mannose and dextran, remarkably improved active targeting of macrophages and gene transfection efficiency of NPs. In addition, the gene transfection efficiency depended on the type and content of the carbohydrate moieties. It is important to note that the main components of the NPs are FDA approved agents, making the NPs an attractive gene carrier system with clinical translational potential. This work provides a potential and technical platform for the delivery of biomacromolecules and therapeutic genes to macrophages at the site of inflammation, which is an encouraging step towards clinical translation of targeted gene therapy for the treatment of macrophage-mediated inflammatory diseases.

Declaration of Competing Interest

The authors declare no conflict of interest.

Acknowledgments

Xue-Qing Zhang acknowledges the financial supports from Thousand Talents Plan for Young Professionals, the Interdisciplinary Program of Shanghai Jiao Tong University (project number ZH2018ZDA36 (19X190020006)), and Shanghai Jiao Tong University Scientific and Technological Innovation Funds (2019TPA10). Qijing Chen acknowledges the National Natural Science Foundation of China (21801189). We also acknowledge the use of nuclear magnetic resonance spectrometer in Prof. Lei Fu lab, and provision of GFP DNA and EGFP mRNA by Prof. Feng Qian and Prof. Yingjie Xu, respectively.

Appendix A. Supplementary data

Supplementary data to this article can be found online at https://doi.org/10.1016/j.jconrel.2020.03.044.

References

[1] F. Ginhoux, S. Jung, Monocytes and macrophages: developmental pathways and tissue homeostasis, Nat. Rev. Immunol. 14 (2014) 392–404.
[2] D.G. DeNardo, B. Ruffell, Macrophages as regulators of tumour immunity and immunotherapy, Nat. Rev. Immunol. 19 (2019) 369–382.
[3] S. Fujisaka, I.I. Usui, A. Bukhari, M. Ikutani, T. Oya, Y. Kanatani, K. Tsuneyama, Y. Nagai, K. Takatsu, M. Urakaze, M. Kobayashi, K. Tobe, Regulatory mechanisms for adipose tissue M1 and M2 macrophages in diet-induced obese mice, Diabetes 58 (2009) 2574–2582.
[4] D.G. Monica, D. Crean, M. Barry, O. Belton, M1- and M2-type macrophage responses are predictive of adverse outcomes in human atherosclerosis, Front. Immunol. 7 (2016) 275–292.
[5] I. Tabas, Macrophage death and defective inflammation resolution in atherosclerosis, Nat. Rev. Immunol. 10 (2010) 36–46.
[6] M. He, Z. Xu, T. Ding, D.M. Kuang, L. Zheng, MicroRNA-155 regulates inflammatory cytokine production in tumor-associated macrophages via targeting C/EBPβ, Cell. Mol. Immunol. 6 (2009) 343–352.
[7] N. Somia, I.M. Verma, Gene therapy: trials and tribulations Nat, Rev. Gen. Therm. 1 (2000) 91–99.
[8] C.D. Thompson, M.R. Frazier-Jessen, R. Rawat, R.P. Nordan, R.T. Brown, Evaluation of methods for transient transfection of a murine macrophage cell line, RAW264.7, Bio. Tech. (1999) 824–832.
[9] K.A. Whitehead, J.R. Dorkin, A.J. Vegas, P.H. Chang, O. Veiseh, J. Matthews, O.S. Fenton, Y. Zhang, K.T. Olejnik, V. Yesilyurt, D. Chen, S. Barros, B. Klebanov, T. Novobrantseva, R. Langer, D.G. Anderson, Degradable lipid nanoparticles with predictable *in vivo* siRNA delivery activity, Nat. Commun. 5 (2014) 4277.
[10] T.T. Smith, S.B. Stephan, H.F. Moffett, L.E. McKnight, W. Ji, D. Reiman, E. Bonagofski, M.E. Wohlfahrt, S.P.S. Pillai, M.T. Stephan, In situ programming of leukaemia-specific T cells using synthetic DNA nanocarriers, Nat. Nanotechnol. 12 (2017) 813–820.
[11] P.Y. Teo, C. Yang, J.L. Hedrick, A.C. Engler, D.J. Coady, S. Ghaem-Maghami, A.J. George, Y.Y. Yang, Hydrophobic modification of low molecular weight polyethylenimine for improved gene transfection, Biomaterials 34 (2013) 7971–7979.
[12] J. Wang, F. Meng, B.K. Kim, X. Ke, Y. Yeo, In-vitro and in-vivo difference in gene delivery by lithocholic acid-polyethyleneimine conjugate, Biomaterials 217 (2019) 119296–119304.
[13] R.A. Ezekowitz, D.J. Williams, H. Koziel, M.Y. Armstrong, A. Warner, F.F. Richards, R.M. Rose, Uptake of Pneumocystis carinii mediated by the macrophage mannose receptor, Nature 6322 (1991) 155–158.
[14] C.M. Paulos, M.J. Turk, G.J. Breur, P.S. Low, Folate receptor-mediated targeting of therapeutic and imaging agents to activated macrophages in rheumatoid arthritis, Adv. Drug Deliv. Rev. 56 (2004) 1205–1217.
[15] Z. Liu, M. Xiong, J. Gong, Y. Zhang, N. Bai, Y. Luo, L. Li, Y. Wei, Y. Liu, X. Tan, R. Xiang, Legumain protease-activated TAT-liposome cargo for targeting tumours and their microenvironment, Nat. Commun. 5 (2014) 4280–4291.
[16] T. Ferkol, J.C. Perales, F. Mularo, R.W. Hanson, Receptor-mediated gene transfer into macrophages, Proc. Natl. Acad. Sci. U. S. A. 93 (1996) 101–105.
[17] S. Kawakami, A. Sato, M. Nishikawa, F. Yamashita, M. Hashida, Mannose receptor-mediated gene transfer into macrophages using novel mannosylated cationic liposomes, Gene Ther. (2000) 292–299.
[18] K. Un, S. Kawakami, R. Suzuki, K. Maruyama, F. Yamashita, M. Hashida, Enhanced transfection efficiency into macrophages and dendritic cells by a combination method using mannosylated lipoplexes and bubble liposomes with ultrasound exposure, Hum. Gene Ther. 21 (2009) 65–74.
[19] P. Erbacher, M.T. Bousser, J. Raimond, M. Monsigny, P. Midoux, A.C. Roche, Gene transfer by DNA-glycosylated polylysine complexes, Hum. Gene Ther. 7 (1996) 721–729.
[20] S. Dokka, D. Toledo, X. Shi, J. Ye, Y. Rojanasakul, High-efficiency gene transfection of macrophages by lipoplexes, Int. J. Pharm. 206 (2000) 97–104.
[21] H.L. Jiang, M.L. Kang, J.S. Quan, M.L. Kang, T. Akaike, H.S. Yoo, C.S. Cho, The potential of mannosylated chitosan microspheres to target macrophage mannose receptors in an adjuvant-delivery system for intranasal immunization, Biomaterials 29 (2008) 1931–1939.
[22] A. Sato, S. Kawakami, M. Yamada, F. Yamashita, M. Hashida, Enhanced gene transfection in macrophages using mannosylated cationic liposome-polyethylenimine-plasmid DNA complexes, J. Drug Target. 9 (2010) 201–207.
[23] J.M. Irache, H.H. Salman, C. Gamazo, S. Espuelas, Mannose-targeted systems for the delivery of therapeutics, Expert Opin. Drug Deliv. 5 (2008) 703–724.
[24] D.S. Surasi, J. O'Malley, P. Bhambhvani, 99mTc-tilmanocept: a novel molecular agent for lymphatic mapping and sentinel lymph node localization, J. Nucl. Med. Technol. 43 (2015) 87–91.
[25] L. Ma, T.W. Liu, M.A. Wallig, I.T. Dobrucki, L.W. Dobrucki, E.R. Nelson, K.S. Swanson, A.M. Smith, Efficient targeting of adipose tissue macrophages in obesity with polysaccharide nanocarriers, ACS Nano 10 (2016) 6952–6962.
[26] X.Q. Zhang, O. Even-Or, X. Xu, M.V. Rosmalen, L. Lim, S. Gadde, O.C. Farokhzad, E.A. Fisher, Nanoparticles containing a liver X receptor agonist inhibit inflammation and atherosclerosis, Adv. Healthc. Mater. 4 (2015) 228–236.
[27] M.A. Islam, Y. Xu, W. Tao, J.M. Ubellacker, M. Lim, D. Aum, G.Y. Lee, K. Zhou, H. Zope, M. Yu, W. Cao, J.T. Oswald, M. Dinarvand, M. Mahmoudi, R. Langer, P.W. Kantoff, O.C. Farokhzad, B.R. Zetter, J. Shi, Restoration of tumour-growth suppression *in vivo* via systemic nanoparticle-mediated delivery of PTEN mRNA, Nat. Biomed. Eng. 2 (2018) 850–864.
[28] X. Xu, K. Xie, X.Q. Zhang, E.M. Pridgen, G.Y. Park, D.S. Cui, J. Shi, J. Wu, P.W. Kantoff, S.J. Lippard, R. Langer, G.C. Walker, O.C. Farokhzad, Enhancing tumor cell response to chemotherapy through nanoparticle-mediated codelivery of siRNA and cisplatin prodrug, Proc. Natl. Acad. Sci. U. S. A. 110 (2013) 18638–18643.